Molecular Therapy
Original Article

Autologous Cell Therapy Approach for Duchenne Muscular Dystrophy using PiggyBac Transposons and Mesoangioblasts

Pavithra S. Iyer,[1,7] Lionel O. Mavoungou,[1] Flavio Ronzoni,[2] Joanna Zemla,[3] Emanuel Schmid-Siegert,[4] Stefania Antonini,[5] Laurence A. Neff,[6] Olivier M. Dorchies,[6] Marisa Jaconi,[2] Malgorzata Lekka,[3] Graziella Messina,[5] and Nicolas Mermod[1]

[1]Institute of Biotechnology, University of Lausanne, Lausanne, Switzerland; [2]Department of Pathology and Immunology, Faculty of Medicine, University of Geneva, 1211 Geneva, Switzerland; [3]Institute of Nuclear Physics, Polish Academy of Sciences, 31342 Krakow, Poland; [4]Swiss Institute of Bioinformatics, Lausanne, Switzerland; [5]Department of Biosciences, University of Milan, 20133 Milan, Italy; [6]School of Pharmaceutical Sciences, University of Geneva and University of Lausanne, 1211 Geneva, Switzerland

Duchenne muscular dystrophy (DMD) is a lethal muscle-wasting disease currently without cure. We investigated the use of the PiggyBac transposon for full-length dystrophin expression in murine mesoangioblast (MABs) progenitor cells. DMD murine MABs were transfected with transposable expression vectors for full-length dystrophin and transplanted intramuscularly or intra-arterially into *mdx*/SCID mice. Intra-arterial delivery indicated that the MABs could migrate to regenerating muscles to mediate dystrophin expression. Intramuscular transplantation yielded dystrophin expression in 11%–44% of myofibers in murine muscles, which remained stable for the assessed period of 5 months. The satellite cells isolated from transplanted muscles comprised a fraction of MAB-derived cells, indicating that the transfected MABs may colonize the satellite stem cell niche. Transposon integration site mapping by whole-genome sequencing indicated that 70% of the integrations were intergenic, while none was observed in an exon. Muscle resistance assessment by atomic force microscopy indicated that 80% of fibers showed elasticity properties restored to those of wild-type muscles. As measured *in vivo*, transplanted muscles became more resistant to fatigue. This study thus provides a proof-of-principle that PiggyBac transposon vectors may mediate full-length dystrophin expression as well as functional amelioration of the dystrophic muscles within a potential autologous cell-based therapeutic approach of DMD.

INTRODUCTION

Duchenne muscular dystrophy (DMD) is a lethal X-linked muscular dystrophy affecting 1 in 5,000 boys.[1,2] DMD results from various types of mutations in the dystrophin gene that lead to progressive muscle wasting, cardiomyopathy, and respiratory failure.[3] Despite several research approaches to find a potential cure for the disease, success remains modest. The current palliative care for patients includes the use of anti-inflammatory drugs and corticosteroids, which have been shown to prolong life expectancy to about 30 years of age.[4] Dystrophin provides a physical link between the cytoskeleton of the muscle fiber and the extracellular matrix, and it is required for the assembly and maintenance of the dystroglycan complex.[5] The absence of this protein causes muscle fiber degeneration, inflammation, and necrosis, and progressive replacement of muscle with scar and fat tissue. Among the potential treatment strategies that were assessed, exon skipping is one of the most advanced today.[5,6] Exon-skipping techniques are promising for the treatment of many types of mutations affecting dystrophin, allowing the skipping of single or multiple exons. This method is expected to convert the severe dystrophic phenotype of DMD patients into milder Becker muscular dystrophy-like phenotypes; however, it may not be suitable to treat all DMD-causing mutations.[7,8]

Cell transplantation-based approaches were also attempted. Skeletal muscle fibers are multi-nucleated; hence, restoring dystrophin expression in one nucleus may provide functional restoration of the entire muscle fiber.[9] However, muscles are among the most abundant tissues of the body, and systemic correction might require the engraftment of billions of cells. Gene-transfer-based approaches are limited by the large size of the dystrophin coding sequence, by transgene silencing issues, as well as by the difficulty of mediating systemic and sustained dystrophin expression.[10] A 11.1-kb open reading frame is required to encode the 427-kDa full-length protein, which is difficult to integrate into lenti- and retro-viral gene therapy vectors. Thus, *in vivo* gene therapy has been attempted using helper-dependent adenoviral vectors that may carry the full-length dystrophin coding sequence but show limitations with respect to mediating therapeutic

Received 21 June 2017; accepted 29 January 2018;
https://doi.org/10.1016/j.ymthe.2018.01.021.

[7]Present address: Department of Chemistry and Applied Biosciences, ETH Zurich, 8093 Zürich, Switzerland

Correspondence: Nicolas Mermod, Laboratory of Molecular Biotechnology, Station 6, FSB-ISP-EPFL, 1015 Lausanne, Switzerland.
E-mail: nicolas.mermod@unil.ch

dystrophin levels in the entire musculature. Adeno-associated viral (AAV) vectors are another attractive option for efficient systemic delivery in the muscles; however, their use is hampered by their restricted packaging capacity.[11] Human artificial chromosome vectors provide another approach toward the expression of the entire dystrophin coding sequence but face the difficulty of inefficient production and delivery.[12,13]

Gene-editing approaches using CRISPR-Cas9 system have also being explored in mouse models; however, they cannot be used efficiently to correct large deletions, which form a majority of the mutations in patients, and efficacy on large populations of cultured cells remains limiting.[14–17] Other pursued alternative approaches consist of the use of truncated versions of the dystrophin sequence encoding micro- or mini-dystrophin proteins and the upregulation of utrophin, the homolog of dystrophin.[18–22]

Transposable vectors stably integrate their cargo into permissive regions of the target cell genome, hence enabling long-term expression of the therapeutic genes.[23,24] For instance, the Sleeping Beauty transposon system has been used for the expression of micro-dystrophin, a shortened version of dystrophin, and dysferlin in muscle dystrophy murine models, and it was optimized for use in a clinical setting.[25–27] PiggyBac (PB) transposons, originally identified in the cabbage looper moth *Trichoplusia ni*, are also able to efficiently transpose in mammalian cells with a large cargo DNA capacity, and PB-derived vectors were shown to mediate stable expression of full-length dystrophin.[28] They combine the easier production of non-viral vectors with efficient transposition and sustained expression in a broad variety of cell types.[29] Although transposons share the limitations of other non-viral vectors regarding a less-efficient intracellular delivery relative to viral vectors, they are among the most promising non-viral vectors for gene therapy applications because of their versatility. PB transposon vectors typically consist of transposon donor plasmids containing a therapeutic gene flanked by the PB transposon inverted terminal repeat (ITR) sequences. They are provided together with a distinct source of the PB transposase, which binds the ITR and mobilizes the transposable vector to mediate genomic integration by a cut-and-paste mechanism.[30]

Here, we aimed at investigating an autologous cell therapy approach based on full-length dystrophin expression in mesoangioblasts (MABs), as PB transposon vectors were previously found to yield stable transgene expression in these cells.[28,31] MABs are progenitor cells associated with blood vessels that are able to differentiate into several mesenchymal tissues, including skeletal muscle.[32] These cells are an attractive option for cell therapy, as they are relatively easy to isolate and culture *in vitro*, they retain their differentiation properties after culture, they efficiently differentiate into muscle cells in the context of damaged muscle tissues, and they are able to cross blood vessel walls, hence making systemic distribution and migration to regenerating muscle possible.[33,34] MABs were shown to infiltrate dystrophic muscle from the circulation, engraft into host fibers with high efficiency, and bring along therapeutic genes and proteins. MABs provide such effect either by direct fusion with the muscle fibers or by entering the muscle satellite cell niche.[12,34] These are promising properties for the systemic and sustained treatment of muscular dystrophies such as DMD. Given their therapeutic potential to improve muscle structure and function in a large animal model, allogeneic MAB transplantation was used in a clinical trial, demonstrating the safety of this approach; however, there was no improvement in phenotype after this transplantation.[34,35]

In this study, we wished to establish the use of the native PB transposon vectors for the expression of full-length dystrophin in MABs and to assess the therapeutic potential of these MABs following transplantation in the mouse model of DMD. We show that PB-mediated dystrophin-coding sequence delivery in *mdx* mouse MABs, followed by cell transplantation into dystrophic *mdx*/SCID mice, led to dystrophin expression in mouse muscles and to morphological and functional amelioration of the dystrophic phenotype in *mdx*/SCID mice.

RESULTS

Characterization of *mdx* MABs Corrected Using Transposable Vectors

The strategy assessed in the present study involved the isolation of MABs from *mdx* mice and their transfection using the non-viral PB transposon vectors expressing dystrophin and/or a reporter gene. This was followed by transplantation of the selected myogenic progenitors into dystrophic mouse muscles, and by the characterization of the transplanted cells and muscles for morphological and functional amelioration of the dystrophic phenotype, as summarized in Figure 1.

PB transposon donor plasmids were constructed to express the full-length human dystrophin coding sequence, under control of a truncated muscle creatine kinase (MCK) promoter. A GFP or nlacZ reporter gene under control of a constitutive glyceraldehyde 3-phosphate dehydrogenase (GAPDH) promoter was expressed on a separate transposon donor plasmid. The PB transposase was expressed from another plasmid under control of the simian cytomegalovirus IE94 promoter, as performed in a previous study showing that transposase expression-mediated sustained reporter gene expression from transposable vectors in murine muscles.[31]

To investigate whether the transposable vector system could restore dystrophin expression in the DMD mouse model, we first isolated MABs from *mdx* mice (*mdx* MABs). The dystrophin and GFP or lacZ-expressing transposon donor plasmids were introduced in *mdx* MABs together with the transposase-encoding plasmid by electroporation. Cells having integrated dystrophin and/or reporter transgenes into their genome were selected by puromycin antibiotic resistance. These cells were called *mdx* (DYS GFP/nlacZ PB) MABs according to the integrated transgenes (Figure 2A). These polyclonal cell populations were characterized for the maintenance of MAB cell markers and for their differentiation and migration potential *in vitro* (Figures 2B–2E and S1). The *mdx* (DYS PB) MABs also retained the different regions of the human dystrophin coding sequence, as

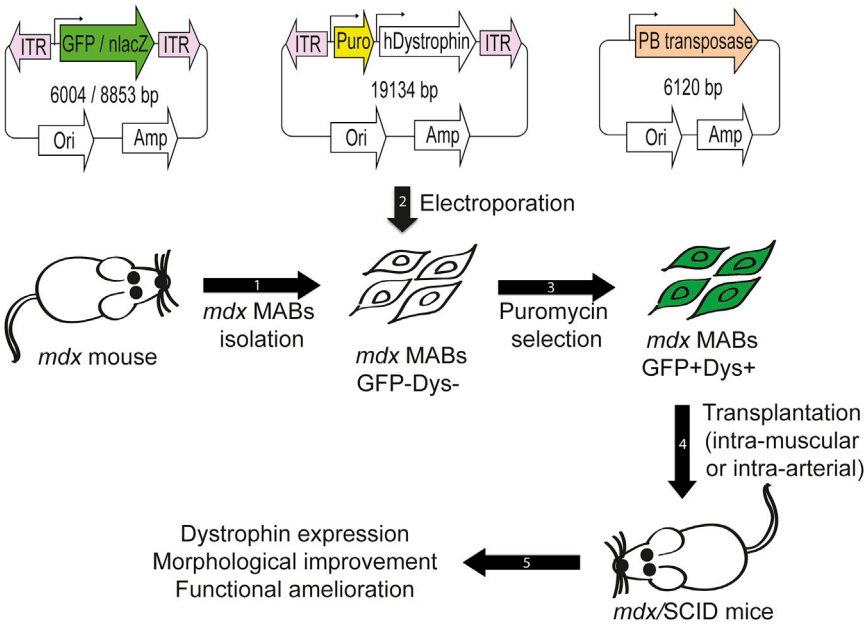

Figure 1. Strategy Used for Genetic Modification of *mdx* MABs and Transplantation in *mdx*/SCID Mice

(1) Isolation of *mdx* MABs from muscles of *mdx* mice. (2) Electroporation of transposon donor plasmids (harboring human dystrophin and/or the GFP or nlacZ reporter) and transposase plasmids shown in the top part of the figure panel. (3) Selection of polyclonal MAB populations by culture in the presence of puromycin for 3 weeks. These modified and selected *mdx* MABs are called *mdx* (DYS PB) MABs, *mdx* (DYS GFP PB) MABs, or *mdx* (DYS nlacZ PB) MABs, depending on whether they were transfected with the dystrophin (DYS), green fluorescent protein (GFP), nucleus-targeted beta-galactosidase (nlacZ), and/or transposase (PB) expression vectors. (4) After *in vitro* characterization, genetically modified and selected MABs were transplanted in *mdx*/SCID mice either IM or IA. (5) Analysis of dystrophin expression and of the morphological and functional amelioration of the transplanted muscles.

verified by endpoint PCR (Figure 2F). Differentiation of *mdx* MABs *in vitro* when co-cultured with mouse C2C12 myoblasts was assessed by the staining the differentiated myotubes with anti-myosin heavy-chain antibody and by observing GFP positive myotubes (Figure 2B). The genetically modified *mdx* MABs retained their morphology, migration, and differentiation properties, and their cell surface markers were comparable to those of the parent *mdx* MABs, as assessed by flow cytometry or by transcript level analysis (Figures 2C and 2D). These properties did not vary along culture passages (data not shown).

Cell survival following transfection and the transposition efficiency were assessed, indicating that 0.226% of the transfected cell population had survived transfection and had integrated at least one transgene copy in the presence of the transposase, whereas the spontaneous plasmid integration frequency observed in the absence of the transposase was much lower (0.026%; see Figures S2A–S2C). The overall pattern of transposable vector mediated transgene integration in the MAB genome was assessed by sequencing the genomes of a polyclonal population of *mdx* (DYS PB) MABs. Transposon integration sites were identified from the sequencing reads spanning both the genome and vector. This approach led to the recovery of 44 distinct integration sites spread over 17 chromosomes of the mouse genome, without a detectable preference for specific chromosomes or genomic loci, as illustrated in Figure 3A. Seventy percent of the integration sites were in intergenic regions, and all integration sites within genes were found to be intronic, none was located in an exon (Figure 3B). To investigate if integrations occurred with a preference for upstream regulatory regions such as promoters or enhancers, the occurrence of integration events was plotted relative to the nearest gene sequence and orientation. Most integration sites were scattered beyond 1 kb upstream or downstream of coding sequences, with just 11% of the integrations within 1,000 bp of a transcription initiation site (Figures 3B and 3C). The total number of integration sites per genome was also assessed using qPCR, using both a standard calibration method and comparison to a reference cellular gene for normalization, in addition to whole-genome sequencing. These methods revealed between two and six integration events per MAB haploid genome (Figure S2D). Overall, these results were consistent with previous findings that few transposon integration events can lead to sustained transgene expression.[31]

Dystrophin Expression from *mdx* (DYS GFP/nlacZ PB) MABs Muscle Transplantation

To assess whether the corrected MABs would engraft and differentiate into muscle fibers *in vivo*, *mdx* (DYS GFP PB) MABs were transplanted in dystrophic immunodeficient (*mdx*/SCID) mice, to avoid immune rejection due to the expression of the human dystrophin and reporter genes. Approximately 500,000 cells were transplanted intramuscularly in the tibialis anterior (TA) muscle of *mdx*/SCID mice, either as a single transplant or as three successive transplants at an interval of 3 weeks, after a pretreatment of the muscles with cardiotoxin 24 hr prior to the first MAB intramuscular injection, to better mimic the more severe condition of the muscles of human dystrophic patients. Single-transplanted mice were assessed at 45 days (short term) or 120 days (long term) after transplant, and three-time transplanted mice were assessed 45 days after the last transplant. All the transplanted muscles showed extensive GFP-positive areas when observed under a fluorescence microscope (Figure S3). Muscle cross-sections showed the presence of extensive areas of dystrophin-positive fibers, with correct sarcolemmal membrane localization, which indicated extensive engraftment of donor MABs and sustained dystrophin expression thereafter (Figures 4A, S4, top panel, and S5). Quantification of dystrophin-positive fibers in serial cross-sections showed between 200 and 800 dystrophin-positive fibers in single transplanted muscles (short and long term), and 300 to 2,500 positive fibers in the muscles transplanted three times

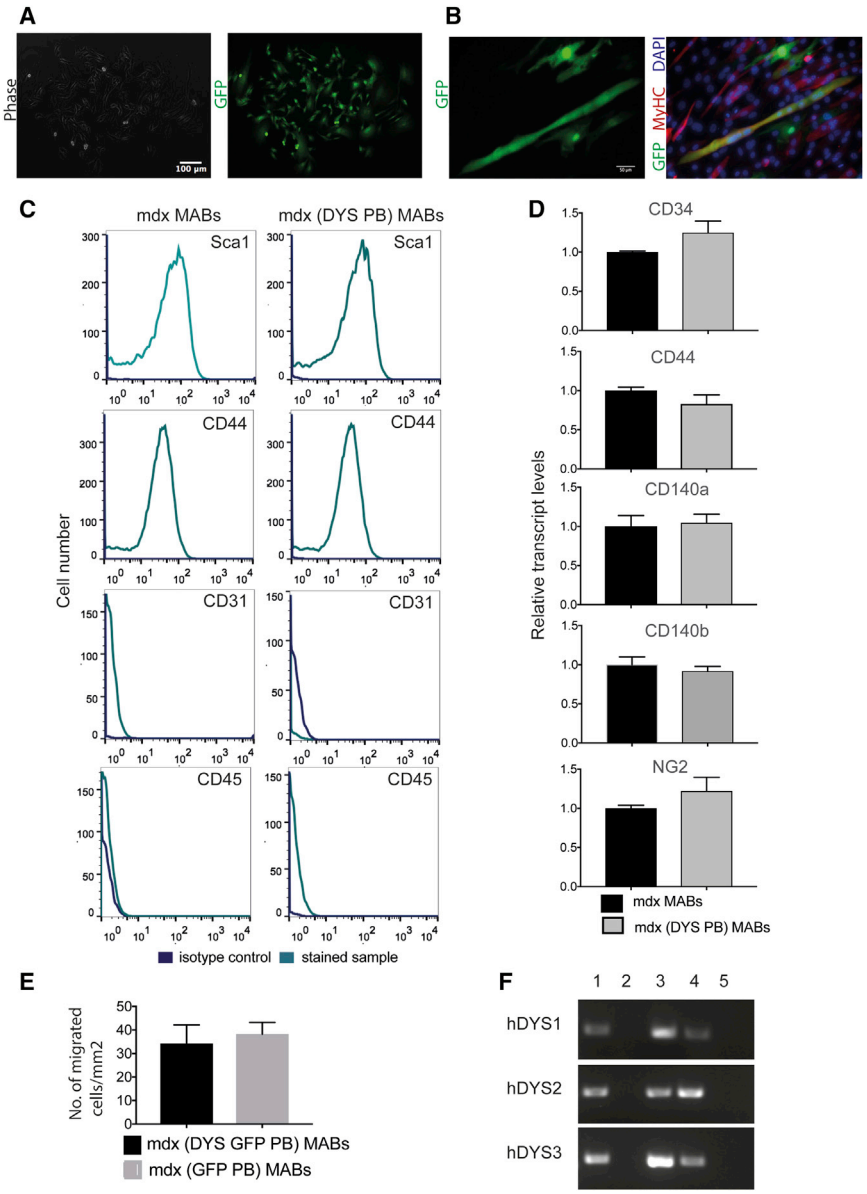

Figure 2. Characterization of *mdx* MABs Carrying Dystrophin- and GFP-Expressing PB Transposons

(A) Phase contrast (left) and fluorescence microscopy (right) analysis of *mdx* (DYS GFP PB) MABs transfected with PB transposon harboring dystrophin and GFP expression cassettes and selected for puromycin resistance. Scale bar, 100 µm. (B) *In vitro* differentiation of the *mdx* (DYS GFP PB) MABs by co-culture in differentiation medium with a GFP-negative mouse myoblast (C2C12) cell line. GFP fluorescence (green), with myosin heavy-chain immunofluorescence of myotubes (red) and DAPI nuclear staining (blue, right), was performed after 5 days of culture in differentiation medium showing a multinucleated GFP- and MyHC-positive myotube. Scale bar, 50 µm. (C) Flow cytometry analysis for the presence of MAB cell surface markers on untransfected *mdx* MABs or transfected *mdx* (DYS PB) MABs populations, as indicated (n = 4). (D) Reverse transcriptase and quantitative real-time PCR (real-time qPCR) analysis of relative transcript levels for different MAB markers in *mdx* MABs and *mdx* (DYS PB) MABs. Data are represented as the mean ± SD of three independent experiments, each performed in triplicate (E). *In vitro* transmigration of MABs performed on endothelial cells (H5V cell line) cultured on a gelatin-coated filter. GFP-positive MABs were added on the upper surface of the filters, and after 11 hr, the MABs that had migrated on the other side of the filter were quantified. The number of *mdx* (DYS GFP PB) MABs and *mdx* (GFP PB) MABs normalized to the area is represented as the mean ± SD from three experiments, each performed in triplicate ($p < 0.05$, negative control versus test group). (F) Endpoint PCR analysis showing the presence of different loci (denoted as hDYS1, hDYS2, hDYS3) of the human dystrophin coding sequence in selected and cultured *mdx* (DYS PB) MABs. Lane 1, *mdx* (DYS PB) MABs; lane 2, non-transfected *mdx* MABs; lane 3, dystrophin expression vector; lane 4, human MAB control; lane 5, water control. The results of three independent experiments are shown.

(Figure 4B). This constituted between 3% and 19% of dystrophin-positive fibers in the cross-section in single-transplanted muscles (short and long term), and 11% and 44% of the fibers in muscles transplanted three times. These numbers were clearly higher than those of the revertant fibers seen in non-transplanted TA muscles, which were 6–10 dystrophin-positive fibers per muscle cross-section. The number of dystrophin-positive fibers remained at similar levels in the mid-belly of the transplanted muscles (5 to 8 mm from the distal tendon) in all the transplant conditions, revealing that there may be fiber length expression in some of the dystrophin-positive fibers (Figure 4B). Interestingly, the number of dystrophin-positive fibers observed after a single transplant remained stable even up to 4 months after transplantation (Figure 4D).

Semiquantitative analysis of dystrophin signal intensity, as assessed by immunofluorescence and confocal microscopy, revealed that the dystrophin signal intensity of areas with a high proportion of dystrophin-positive myofibers in treated muscles was similar to that of wild-type mouse muscles (Figure S6). Also, immunofluorescence analysis of transplanted muscles showed reconstitution of the dystrophin protein complex, as evidenced with α-sarcoglycan, β-sarcoglycan, β-dystroglycan, syntrophin, and neuronal nitric oxide synthase (nNOS) (Figure S7). RT-PCR analysis confirmed correct expression of the muscle isoform of dystrophin (Dp427m) (Figure S8), and RT-qPCR showed that dystrophin transcript accumulation in the muscles was increased approximately three-fold after three transplantations (Figure 4E). Similar observations were found by qPCR analysis of DNA from transplanted muscles, where DNA levels of the dystrophin vector were approximately three times higher in muscles transplanted three times than those of single-transplanted

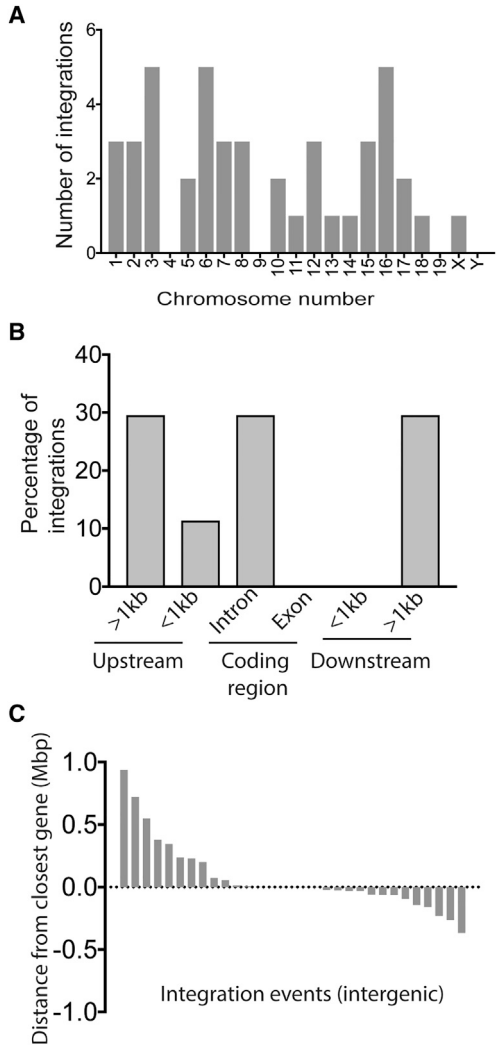

Figure 3. Integration Site Profile of Transposon in *mdx* (DYS PB) MABs

(A) Distribution of integration sites over the different chromosomes to assess a possible transposition preference. (B) Graph showing the percentage of integrations in introns, exons, and in different parts of intergenic regions (<1 kb upstream or downstream of coding sequences; >1 kb upstream or downstream of coding sequences), n = 44. (C) Mapping of intergenic integration events based on their distance from the closest gene. Upstream or downstream transposition events are indicated by negative or positive numbers, respectively. Each bar denotes an individual intergenic integration event.

muscles at short time point (Figure 4C), suggesting improved engraftment upon successive transplantations. However, transposase DNA levels were essentially undetectable in the transplanted muscles, implying a low risk of *in vivo* transposition events post-engraftment. Assessment of backbone plasmid DNA levels by qPCR also indicated almost undetectable levels, consistent with mainly transposon-mediated cargo DNA integrations (Figure 4C). Moreover, western blot analysis showed that transplanted muscles expressed 20%–40% of dystrophin levels as compared to non-dystrophic B6/SCID mice, as estimated from densitometry analysis of western blots, which correlates well with the proportion of dystrophin-expressing myofibers (Figure 4F).

Because the diffuse GFP signal was not readily detected in cross-sections following MAB muscle transplantation, we next used the nuclear localized nLacZ reporter coding sequence. Upon intra-arterial transplantation of *mdx* (DYS nlacZ PB) MABs into the femoral artery of *mdx*/SCID mice, small clusters of dystrophin-positive fibers were observed in the gastrocnemius muscle cross-sections (35–45 dystrophin-positive fibers/cross-section) 4 weeks after transplant (Figure S4, lower panel). A few nLacZ$^+$ nuclei were also visible in the interstitium in other areas of the grafted muscles, but their numbers were too low to be reliably quantified. These numbers are in agreement with previously reported results of intra-arterial MAB transplantation.[12] These results established that the transposon-modified MABs retained their ability to migrate through the vasculature and engraft into regenerating muscles upon systemic transplantation, although the numbers of dystrophin-positive fibers were lower than those obtained from intramuscular injection.

Overall, it was noteworthy that dystrophin expression levels after intramuscular transplantation were maintained at essentially constant levels at the longest time point assessed, 4 months after transplantation, and that the dystrophin DNA, RNA levels, and number of dystrophin-positive fibers in muscles transplanted three times was 3-fold higher than those of single-transplanted muscles. Overall, these data indicated that the genetically modified MABs were able to engraft into murine muscles and to mediate dystrophin expression, which in turn was able to restore the proper localization of the other components of the dystroglycan complex.

Transplanted MABs Seed the Satellite Cell Compartment

In order to examine whether transplanted MABs are able to contribute to the muscle satellite cell pool, we transplanted (DYS nlacZ PB) MABs intramuscularly into *mdx*/SCID mice. Two months after cell transplantation, muscle cross-sections were stained with Pax7 (satellite cell marker), laminin, and β-galactosidase antibodies. A fraction of the β-galactosidase-positive cells were found to display some characteristics of satellite cells, being associated to the basal lamina of transplanted muscles and displaying Pax7 expression (Figure 5A).[12] Hence, the transplanted *mdx* (DYS nlacZ PB) MABs may have retained the ability to colonize the satellite cell niche of the muscle. Muscle satellite cells were also isolated from muscles transplanted with *mdx* (DYS GFP PB) MABs by flow cytometry, showing that approximately 3% of the Int$\alpha7^+$, Sca-1$^-$, CD31$^-$, CD45$^-$, CD11b$^-$ cells were also GFP positive and thus originated from the donor MABs in the muscles transplanted three times (Figures 5B, 5C, S9, and S10). This was significantly higher than the 0.12% of such cells in single-transplanted muscles. A possible reason for this observation may be that the MABs of the first transplant may preferentially fuse with the distressed dystrophic myofibers, whereas the MABs

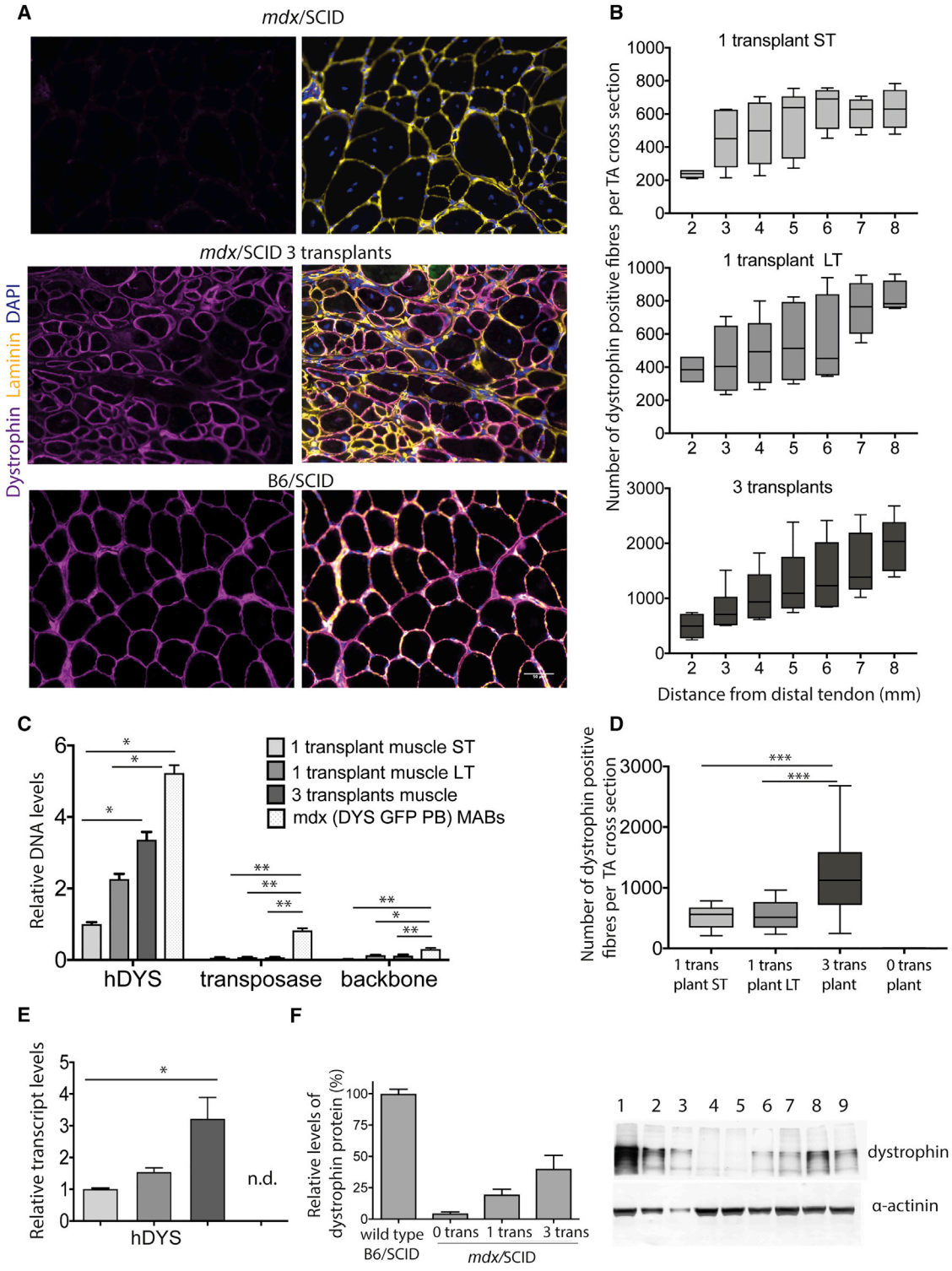

Figure 4. Dystrophin Expression following IM Transplants

Muscles were analyzed either after 45 days (short term, ST) or 120 days (long term, LT) after a single transplant or 45 days after the last of three transplants performed at intervals of 3 weeks. (A) Cross-sections of *mdx*/SCID mouse TA muscles are shown for a mock-transplanted muscle (top) or for a muscle transplanted three times with *mdx*

(legend continued on next page)

delivered during the second and third transplantations may lead to the almost 25-fold increase in the MAB-derived population of satellite-like cells.

The satellite-like cells derived from the transplanted MABs were sorted as based on GFP fluorescence from the Int$\alpha7^+$, Sca-1^-, $CD31^-$, $CD45^-$, and $CD11b^-$ cell population, and they were analyzed for other markers of native satellite cells. The relative transcript levels of the Pax7 and integrin α-7 satellite cell marker genes were comparable in the GFP^+ MAB-derived transplanted cells and in the native satellite cells of non-transplanted muscles (Figure 5D). We concluded that the genetically modified MABs could contribute to both differentiating into muscle fibers as well as to replenishing the pool of muscle progenitor cells, in agreement with previous studies.[12] We therefore hypothesized that the MAB-derived satellite-like cells might contribute dystrophin-positive myofibers in a time-sustained fashion, to possibly reduce the progression of the dystrophic disease.

Morphological Amelioration of Dystrophic Muscles after MAB Transplantation

To understand whether the restoration of dystrophin expression in the transplanted muscles led to a morphological amelioration of the dystrophic phenotype, fibrotic and scar tissue infiltration was quantified, along with the cross-sectional area of individual fibers. The muscles of *mdx*/SCID mice showed the typical infiltration of muscle by mononuclear cells and the replacement of muscle tissue by fibrotic infiltrates and fat tissue (Figure 6A). Cross-sectional areas of individual fibers of the transplanted muscles had reduced variability relative to those of untreated muscles of *mdx/SCID* mice (Figures 6B and S11). Morphometric analyses revealed a marked reduction in the fibrotic and cellular infiltrates of transplanted dystrophic muscles, indicating that treated muscle underwent fewer degeneration-regeneration cycles. The overall percentage of muscle area replaced by fibrotic or scar tissue was significantly reduced in the transplanted muscle cross-sections, from 8% to 14% in the non-treated dystrophic muscle to 4% to 10% in the transplanted muscles (Figure 6C).

Functional Amelioration of the Dystrophic Phenotype after MAB Transplantation

To investigate whether engraftment and restoration of dystrophin expression was accompanied by improvement in muscle function, we evaluated the functional properties of transplanted muscles. Previous studies indicated that atomic force microscopy (AFM) nanoindentation assays are capable of detecting changes in the resistance to elastic deformation of individual myofibers within muscle explants, as evoked by the presence or absence of dystrophin at the sarcolemmal membrane.[36,37] Six weeks after a single or three consecutive intramuscular transplantations, myofiber elasticity was probed on longitudinal sections of TA muscles on randomly chosen myofibers at over 100 locations.

The myofiber resistance to elastic deformation was quantified through Young's modulus value (E), which for dystrophin-expressing B6/SCID control muscles was 18.1 ± 9.9 kPa (Figure 7A). Significantly lower ($p < 0.001$) Young's modulus of 8.5 ± 5.3 kPa was obtained for *mdx*/SCID muscles, indicating lower resistance to applied pressure, as expected.[36,37] The Young's modulus, i.e., the resistance to deformation, of single-transplanted muscles was not significantly higher than those of *mdx*/SCID muscles (9.6 ± 4.8 kPa). However, after three MAB transplantations, a bimodal distribution of the Young's modulus values was observed, with a subpopulation of myofibers having elasticity similar to those of control non-dystrophic muscles (17.2 ± 4.2 kPa; Figure 7A). It was possible to infer from this distribution that 80% of the measured fibers had resistance properties similar to healthy muscles, whereas 20% retained the properties of dystrophic myofibers.

Myofibers with a dystrophic or non-dystrophic phenotype were detected as clusters, as was noted for dystrophin expression and for the restoration of dystrophin-associated protein clusters (Figures S4, S5, and S7B). Interestingly, the proportion of myofibers displaying normal elasticity properties was higher than those where dystrophin expression could be detected (80% versus 45%). This is in agreement with the previous observations that low dystrophin expression levels, which are not easily detected by immunofluorescence, may suffice to

(DYS GFP PB) MABs (middle). The bottom panels show the TA cross-section of a non-dystrophic B6/SCID mouse. Muscles were immunostained for dystrophin only (left), and additionally for laminin and DAPI (right), as indicated. Scale bar, 50 μm. (B) Box-and-whisker plots of the number of dystrophin-positive fibers per TA muscle cross-section, generated at the indicated distances in mm from the distal tendon, short term or long term after a single transplant or after three transplants, as indicated. Box-and-whisker plots represent the 50th percentile as the middle line in the box, the 25th and 75th percentile as the top and bottom of the box, respectively, and the smallest and largest values as the top and bottom of the whiskers. (C) DNA levels of human dystrophin, plasmid backbone, and transposase were assessed by qPCR analysis performed on transplanted muscles on *in vitro* selected *mdx* (DYS GFP PB) MABs. All the qPCR values were normalized to those of short-term single-transplant muscles, which were set to one. Data are represented as mean ± SD from more than six muscles per condition, $^*p \leq 0.05$; $^{**}p \leq 0.01$. (D) Boxplot of the overall numbers of dystrophin-positive fibers from measurements performed at all distances from the distal tendon following the different transplant conditions, $^{***}p \leq 0.001$ ($n \geq 6$). (E) Transcript levels of human dystrophin as assessed by qPCR analysis performed on transplanted muscles or *in vitro* selected *mdx* (DYS GFP PB) MABs. All the qPCR values were normalized to those of short-term single-transplant muscles, which were set to one. Data are represented as mean ± SD from more than six muscles per condition, $^*p \leq 0.05$; $^{**}p \leq 0.01$; n.d., not detectable ($n \geq 6$). (F) Western blot showing dystrophin expression in the *mdx*/SCID muscles transplanted one time with *mdx* (DYS PB) MABs, short term (1 trans), or transplanted three times with *mdx* (DYS PB) MABs, 6 weeks after the last transplant (3 trans) versus non-transplanted *mdx* muscles (0 trans) or non-transplanted B6 muscles, using α-actinin expression as control. Lanes 1 to 3, wild-type B6/SCID control (30 μg; 9 μg and 3 μg protein loaded, respectively); lanes 4 and 5, *mdx*/SCID mock-injected (30 μg); lanes 6 and 7: *mdx*/SCID three transplants (*mdx* [DYS PB] MABs) TA muscles (30 μg); lanes 8 and 9, *mdx*/SCID one transplant (*mdx* [DYS PB] MABs) TA muscles (30 μg). The graph shows the corresponding densitometry analysis of the western blot where values are expressed relative to the total dystrophin levels of wild-type muscles, which were set to 100%.

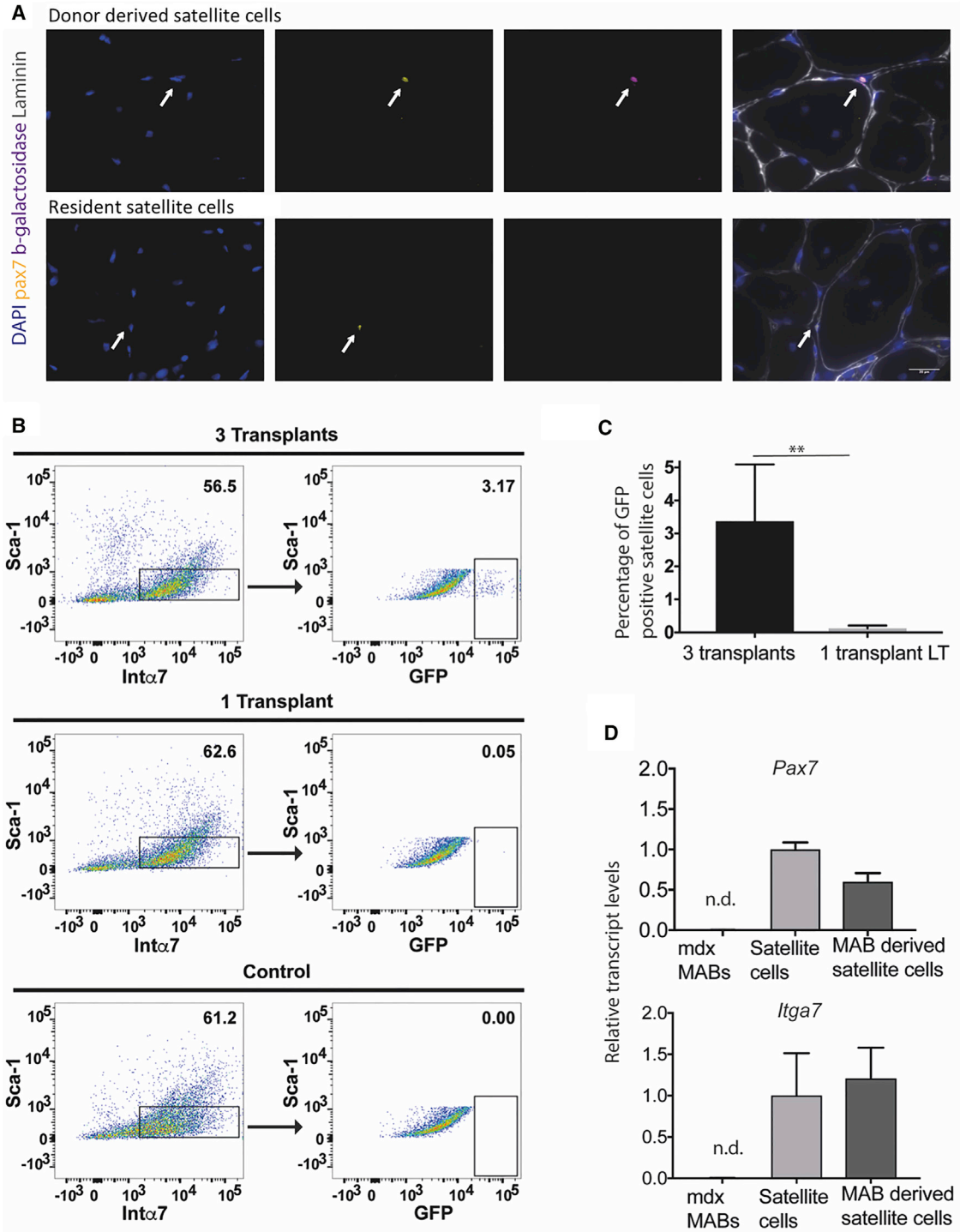

Figure 5. Reconstitution of the Satellite Cell Niche by Donor MABs in IM Transplanted Muscles

(A) Immunofluorescence staining images showing Pax7 staining for satellite cells and β-galactosidase staining for transplanted *mdx* (DYS nLacZ PB) MABs. Top panels show the co-localization of a Pax7 and β-galactosidase staining of positive nucleus under the basal lamina (MAB-derived satellite cell). Bottom panel shows a Pax7 positive nucleus that is not β-galactosidase positive under the basal lamina (resident satellite cell). Scale bar, 20 μm. (B) Fluorescence-based cell sorting of GFP-positive satellite cells (*mdx* DYS GFP PB MAB-derived) and GFP-negative (resident) satellite cells. Boxes in all left panels highlight the proportion of Sca-1$^-$ and Integrin-α7$^+$ cells among the sub-population of CD31$^-$, CD45$^-$, and CD11b$^-$ mononuclear cells, among which the GFP$^+$ cells are boxed on right-hand side panels, i.e., there are 3.17% of GFP$^+$ cells among

(legend continued on next page)

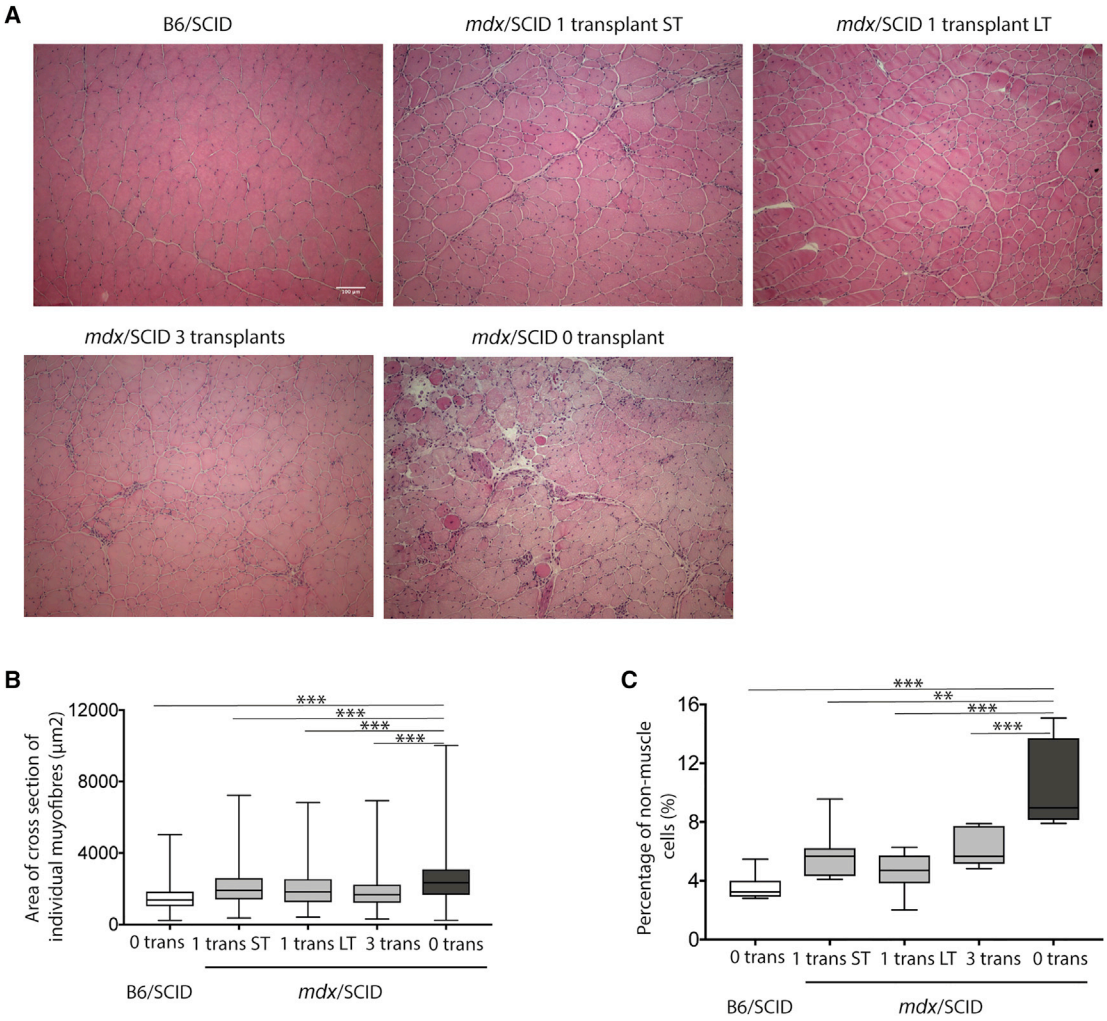

Figure 6. Morphological Amelioration of the Dystrophic Phenotype after IM Transplantation of Genetically Modified MABs

(A) H&E stained images of TA muscle cross-sections of a wild-type B6/SCID mouse, *mdx*/SCID single transplant 6 weeks after transplantation (ST), *mdx*/SCID single transplant 24 weeks after transplantation (LT), *mdx*/SCID three transplants 6 weeks after last transplant, and *mdx*/SCID 0 transplant (mock-injected) muscle. Scale bar, 100 µm. (B) Box-and-whisker plot showing the distribution of the area of individual myofibers, as determined from cross-sections of TA muscles from wild-type B6/SCID mice, *mdx*/SCID single-transplant mice 6 weeks after transplantation (1 trans ST), *mdx*/SCID single-transplant mice 24 weeks after transplantation (1 trans LT), *mdx*/SCID three-transplant mice 6 weeks after last transplant (3 trans), and *mdx*/SCID mock-injected mice (0 trans) ($n \geq 6$). (C) Box-and-whisker plot showing percentage of non-muscle cells (fibrotic and adipose tissue, infiltrating cells) in the different mouse groups. $^{**}p \leq 0.01$; $^{***}p \leq 0.001$ ($n \geq 6$).

restore full myofiber resistance.[38] Thus, immunofluorescence assays likely underestimated the proportion of fibers having elevated dystrophin expression following transplantation.

To further investigate functional restoration in muscles transplanted three times, we performed isometric force measurement on the TA muscles. Tetanic or phasic force parameters were not significantly altered in the transplanted muscles (data not shown). However, MAB transplantation caused a significant restoration of the muscle resistance to fatigue upon repeated tetanic contractions above the untreated *mdx*/SCID muscles (Figures 7B and 7C). Contraction-induced fatigue, a major cause of weakness of dystrophic muscles,

the Sca-1$^-$, Integrin-α7$^+$, CD31$^-$, CD45$^-$, CD11b$^-$ mononuclear cells isolated from the *mdx* SCID mouse muscles after three transplantations. (C) Averages of the percentage of GFP$^+$ satellite cells derived from transplanted *mdx* (DYS GFP PB) MABs from the total population of satellite cells in *mdx*/SCID three-transplant mice, isolated 6 weeks after last transplant, and *mdx*/SCID single transplant 24 weeks after transplantation. Values are expressed as mean ± SD of values from different muscles used for satellite cell isolation (n = 4 for each condition). (D) qPCR analysis of transcript levels of the Pax7 and integrin-α7 satellite cell markers in the resident satellite cell population and donor MAB-derived satellite cells of transplanted muscles; n.d., not detectable.

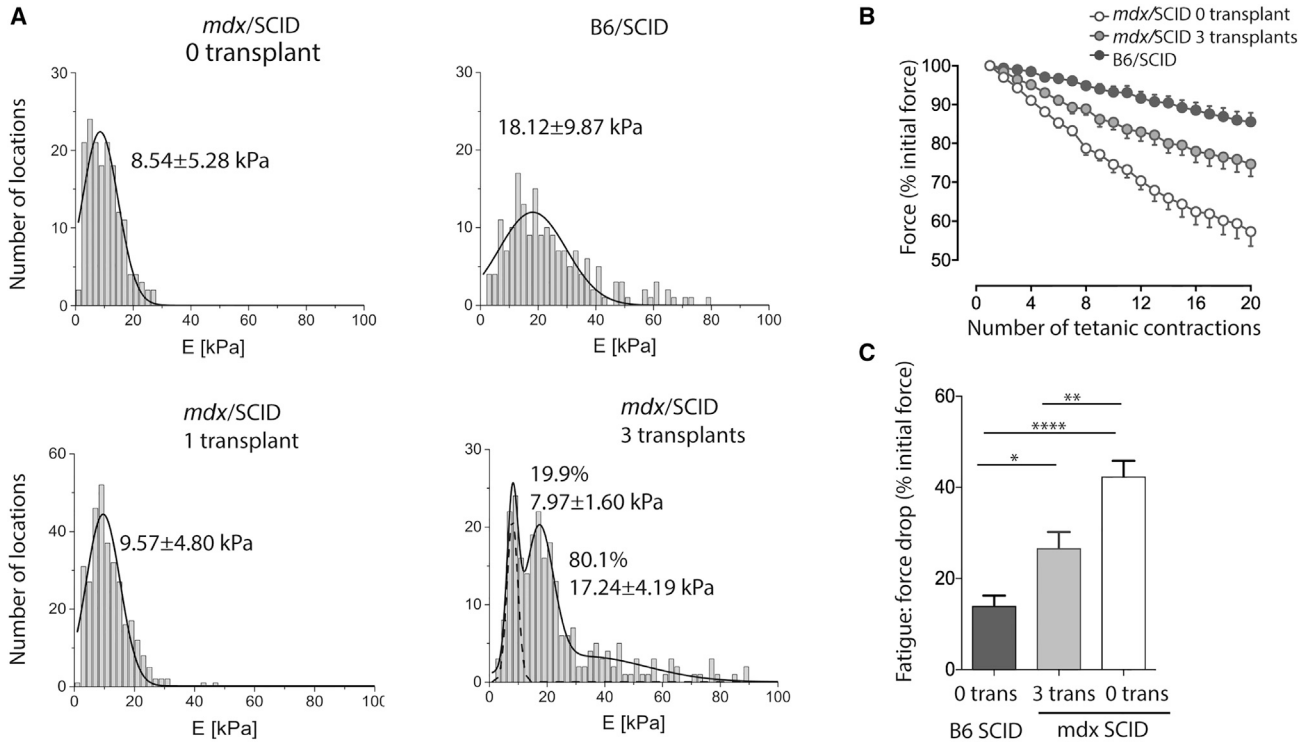

Figure 7. Functional Amelioration of the Dystrophic Phenotype after IM Transplantation of Genetically Modified MABs

(A) AFM-based distributions of Young's modulus (E) obtained for muscles explanted from wild-type B6 SCID mice, *mdx* SCID single-transplant short-term mice 6 weeks after transplantation, mdx SCID three-transplant mice 6 weeks after last transplant, and mdx SCID mock-injected mice. The y axis represents the number of locations assayed, and the x axis denotes Young's modulus value grouped in 2-kPa bins. Gaussian function was fitted to determine the indicated average Young modulus value of each group. n = 8 to 10 muscles per group. (B) Improved muscle function measured *in situ* in living mice. In the TA of wild-type B6/SCID mice, *mdx*/SCID three-transplant mice 6 weeks after last transplant, and *mdx*/SCID mock-injected mice, progressive loss of force was recorded as tetanic stimuli were delivered. This illustrates that mock-injected *mdx*/SCID mice lost force much faster than their wild-type counterparts, and that the *mdx*/SCID mice transplanted three times had a much lower rate of force loss. (C) Improved muscle function measured *in situ* in living mice. Quantification of force loss. Force drop measured at the end of the assay was expressed as percentage of initial force. The force drop in mock-injected *mdx*/SCID mice was 3-fold higher than in the mock-injected B6/SCID mice. The force drop was significantly prevented in *mdx*/SCID mice transplanted three times (recovery index 61.6%). n = 9 to 12 muscles per group. *$p \leq 0.05$; **$p \leq 0.01$; ***$p \leq 0.001$. Data are represented as mean ± SD.

was prevented by more than 60% in muscles injected three times with MABs. Overall, we conclude that the dystroglycan complex and hence the sarcolemmal integrity in the dystrophin-restored regions may be restored in *mdx* myofibers, conferring the transplanted muscles with physical properties similar to those of wild-type muscles and providing an improved resistance to fatigue.

DISCUSSION

Stem cell technologies have the potential to revolutionize medical care as well as provide improved prospects for addressing a host of untreatable muscular dystrophies.[39] The therapeutic potential of muscle stem cells so far has been limited because of their low abundance in adult muscle, and by the fact that *in vitro* expansion of these cells results in reduced engraftment ability.[40] Also, until now, persistent expression of full-length dystrophin in mouse muscles has been difficult to achieve.[12,41] It was recently shown that stable transgene expression can be achieved using PB vectors and MAB transplantation in murine muscles *in vivo* and that the expression of full-length dystrophin could be mediated by such transposable vectors *in vitro*. However, whether this may provide a functional amelioration of dystrophic muscles *in vivo* had not been reported.[28,31] This study shows that MABs modified with PB transposon vectors can yield large numbers of dystrophin-expressing fibers when transplanted into dystrophic immunodeficient mice, and that this leads to a functional improvement of the transplanted muscles, hence fulfilling some of the criteria required for successful cell therapy of muscular dystrophy.

The genetic modification of MABs by PB transposon vectors has several advantages, especially in context of dystrophin, because of their ability to deliver very large DNA cargoes into the genome and to enable stable integration and long-term expression of full-length dystrophin.[28] Also, considering the undesirable aspects of allogeneic transplantation, such as lifelong immune suppression and limited effectiveness, the use of autologous genetically corrected MABs may be a preferred strategy to avoid confronting these issues. An ideal therapeutic strategy would be one in which a full-length

dystrophin-coding sequence would be integrated in non-coding regions of the MAB genome, to allow sufficient transgene expression while avoiding mis-regulation of endogenous cellular genes. Our observations that vector copy number is between two and six per MAB genome, and that 70% of the integrations are in non-coding regions provide significant steps toward this goal. Nevertheless, previous studies have reported that PB transposition events may be favored at transcription start sites and also that vertebrate genomes bear genes distantly related to PB transposase that can nevertheless mobilize the insect PB transposon in human cell cultures when expressed ectopically.[42–44] More extensive analysis will be required to evaluate further the PB integration profile and the risk of potential genotoxicity resulting from these transposable vectors. Several potential improvements to this strategy may be envisaged for potential clinical use, such as further reducing integrated vector copy number, employing other selection strategies than antibiotic resistance, transposon targeting into safe harbors in the genome, e.g., with CRISPR-Cas9, and/or use of a more active transposase. Although we did not observe disruption of any exons in this study, nor did we observe any tumorigenesis from the transposon-containing MABs (data not shown), these additional precautions might be needed to further reduce the potential risk of adverse effects due to insertional mutagenesis or mis-regulation of cellular genes.

The levels of dystrophin protein expression achieved in transplanted muscles was 20% to 40% of the wild-type levels on a whole-muscle basis. However, positive myofibers of transplanted muscles yielded dystrophin expression up to levels that were comparable to those of wild-type muscles. This was sufficient to ameliorate the dystrophic phenotype, as assessed by histological studies, and to restore normal resistance of most *mdx*/SCID myofibers in AFM studies. This is consistent with previous studies, which reported that even moderate dystrophin expression levels can provide improved muscle structure and function.[12,14,15,17,38,45] Such level of dystrophin expression also yielded improved fatigue resistance properties of the treated *mdx*/SCID muscles.

In clinical protocols, systemic delivery may be imperative for fighting the DMD disease, as intramuscular delivery would require an excessive number of injections, including in difficult-to-reach muscles. MABs were previously shown to be able to cross blood vessel walls and to diffuse into—and engraft in—regenerating skeletal muscle when delivered intra-arterially.[12,33,34] This study shows that transposon-containing MABs transplanted into the femoral artery retained ability to migrate across the vessel walls into neighboring muscles where dystrophin-expressing muscle fibers could be detected. However, future studies should seek to further improve the efficiency of IA transplantation and also to determine if these findings can be extrapolated to human MABs, which have similarities and also some differences relative to their murine counterparts.[46]

Taken together, our findings provide a proof-of-concept for the feasibility of combining MAB transplantation with genetic complementation using the PB transposon system for a potential treatment of DMD. This study shows that a fraction of the non-virally corrected *mdx* MABs may have colonized the satellite cell niche upon their engraftment into transplanted muscles. This engraftment could restore dystrophin and dystroglycan protein complex components, thereby mediating morphological amelioration of the dystrophic phenotype, restoring myofiber stiffness to normal levels and improving the muscle resistance to fatigue.

As of today, exon skipping and premature stop codon read-through are among the most advanced innovative strategies for the treatment of DMD. However, a significant proportion of DMD mutations may not be corrected using these approaches. By contrast, autologous cell transplantation using modified MABs carrying the entire dystrophin cDNA may be a promising therapeutic avenue for the treatment of DMD patients bearing any mutation.

MATERIALS AND METHODS

Animal Models and Experimentation

All animal experimentations were done in accordance with institutional guidelines and authorizations for animal research by the State of Vaud veterinary office. *Mdx*/SCID (B10ScSn.Cg-*Prkdc*^{scid} *Dmd*^{mdx}/J) and B6/SCID (B6.CB17-*Prkdc*^{scid}/SzJ) were purchased from Jackson Laboratory (Jackson, Bar Harbor, ME). They were bred and maintained in a specific pathogen-free (SPF) animal facility (University of Lausanne). CD1 nude mice for tumorigenesis assays were purchased from Charles River, France, and housed in an SPF animal facility. Mice were given *ad libitum* access to food and water; the temperature was maintained at 21°C and humidity at 50%–60%. Mice were age, sex, and background matched with their controls for all morphological and functional analysis.

Prior to intramuscular (IM) transplantation, mice were anesthetized with isoflurane and injected IM with cardiotoxin (10 μM, 25 μL), so as to induce muscle regeneration.[47] IM transplantations were done by injecting 500,000 *mdx* (DYS GFP PB/DYS nlacZ PB) MABs resuspended in 25 μL of Ca^{2+} and Mg^{2+} free PBS into the muscles of anesthetized mice using a 30G needle (BD Biosciences). Transplantations were either a single IM transplantation or three consecutive IM transplantations at an interval of 3 weeks, with each injection consisting of 500,000 cells. The muscles from age-, sex-, and background-matched control mice were injected with 25 μL Ca^{2+} Mg^{2+} free PBS. The muscles were explanted and used for various assays at different time points: 45 days after a single transplantation for short-term assays (one transplant ST), 120 days after single transplantation for long-term assays (one transplant LT), or following three transplants 45 days after the last transplant (three transplants).

Intra-arterial (IA) transplantations were performed by injecting 500,000 *mdx* (DYS GFP PB/DYS nlacZ PB) MABs resuspended in 100 μL Ca^{2+} and Mg^{2+} free PBS into the femoral artery of previously exercised mice (flat treadmill to exhaustion allowing the mice to run till they reach fatigue, a day before injection) so as to induce muscle regeneration and to mimic the more severe condition of human DMD patients. The mice were kept under anesthesia (isofluorane,

Attane) while the artery was isolated and cells were injected into the artery, as previously described.[48]

Eight- to ten-week-old male mice were used in the study. The total number of grafted mice for single IM transplantations was 20, whereas it was 40 mice for three consecutive IM transplantations, and eight mice for IA transplantations.

Cell Culture and Plasmids

MABs were isolated from *mdx* mice as previously described.[46] In brief, muscles from 7-day old mice were dissected and minced into 1 mm^2 pieces. These pieces were transferred onto collagen type I-coated dishes (Sigma, St. Louis, MO) and incubated with 50 μL of DMEM culture medium (Gibco, Grand Island, NY) supplemented with 20% fetal bovine serum (FBS) (Lonza, Basel, Switzerland), 2 mM L-glutamine, 1 mM sodium pyruvate, 1× non-essential amino acids, 100 IU/mL penicillin, and 100 mg/mL streptomycin (Gibco, Grand Island, NY). After 7 days, the primary cell outgrowth was collected, and alkaline phosphatase-positive cells (mouse alkaline phosphatase antibody, R&D Systems, Minneapolis, MN) were sorted by FACS (BD FACS Aria II, BD Biosciences, San Jose, CA). This MAB cell population was expanded and maintained at 37°C, 5% CO_2, on collagen-coated plastic dishes. MABs were tested for alkaline phosphatase expression using the Alkaline Phosphatase Live Stain (Molecular Probes, Burlington, Canada), as per the manufacturer's instructions. The live stained cells were observed under a fluorescence microscope for green fluorescence. The MABs were found to be alkaline phosphatase positive, in agreement with their previously reported phenotype (data not shown).[46]

C2C12 mouse myoblasts were maintained in DMEM containing 10% FBS. In order to avoid differentiation, cells were not allowed to reach more than 80% confluence. The differentiation ability of MABs was tested by co-culture with C2C12 cells (2:1 ratio of C2C12 cells to GFP-tagged MABs) for 7 days in differentiation medium (DMEM supplemented with 2% horse serum [Gibco], 2 mM L-glutamine, 100 IU/mL penicillin and streptomycin).[46] The resulting myofibers were stained for myosin-heavy chain MF20 (Thermo Fisher, Waltham, MA) to confirm differentiation into myotubes. For promoting the differentiation of MABs into smooth muscle cells, smooth muscle induction medium (DMEM supplemented with 2% horse serum [Gibco], 2 mM L-glutamine, 1 mM sodium pyruvate, 100 IU/mL penicillin, and 100 μg/mL streptomycin, 5 ng/mL TGFβ1 [Peprotech, Rocky Hill, NJ]).

The PB transposase expression vector has been previously described.[31] In brief, the 3′ UTR 317-bp fragment from pBSSK/SB10 (kindly provided by Dr. S. Ivics) was inserted into pCS2 + U5 (Invitrogen/Life Technologies, Paisley, UK) to yield pCS2 + U5U3. The PB transposase coding sequence (2,067 bp, GenBank accession number, EF587698) was cloned into the pCS2 + U5U3 backbone between the two UTRs. The PB transposon vectors used in the study were generated by introducing the PB 235 bp 3′ and 310 bp 5′ ITRs into the pBluescript SK plasmid. The 11.1-kb human full-length dystrophin coding sequence was kindly provided by J. Tremblay.[49] It was cloned into the PB transposon vector backbone under the previously described MCK promoter.[31,50] A puromycin resistance cassette was introduced into this construct under the control of an SV40 early promoter. Alternatively, a GFP/nlacZ reporter cassette was cloned in the same PB vector under control of the human GAPDH promoter.[31] Endotoxin-free plasmid preparations (QIAGEN endo-free plasmid maxi kit/GeneArt plasmid purification service from Thermo Fisher Scientific) of all the plasmids were used for transfection into *mdx* MABs.

The transposon and transposase expression vectors were introduced by transfection of the MABs using Neon electroporation (Invitrogen, Carlsbad, CA), as per the manufacturer's instructions. One million MABs were co-transfected with 20 μg transposon, 4.5 μg transposase, and 2 μg reporter expression vectors at 1,300 V for two pulses. The metabolic activity and cell survival rates were assessed by Alamar blue staining or propidium iodide dye exclusion assays, respectively, 1 day after transfection. Two days after transfection, the cells were placed in medium containing 2 μg/mL puromycin, and the cells were further cultured for 2 weeks with medium replacement two times per week. Methlylene blue staining of the colonies formed by resistant cells was performed after electroporation and antibiotic selection to determine the transposition efficiency and background levels of random integration. The transfected and selected *mdx* MABs are henceforth called *mdx* (DYS GFP PB), (DYS nlacZ PB), or (DYS PB) MABs, where the transgene names within the parentheses indicate which expression vectors were used, e.g., *mdx* MABs co-transfected with the transposon donor plasmids containing dystrophin coding sequence (DYS) and GFP coding sequence (GFP) and with the transposase expression plasmid (PB) are called *mdx* (DYS GFP PB) MABs.

MABs were prepared for flow cytometry analysis by washing the cells with PBS and staining with antibodies for CD44, Sca-1, CD45, and CD31 conjugated to allophycocyanin or PerCP (R&D Systems) for 1 hour. This was followed by washing again with PBS to remove the excess antibody, and finally the cells were resuspended in PBS supplemented with 2% FBS. The analysis was performed on a Beckman Coulter CyAn ADP (Beckman Coulter, Brea, CA). At least 10,000 events were acquired for each sample.

In vitro cell transmigration assay was performed as previously described.[48] In brief, *mdx* (DYS GFP PB) MABs were cultured on a layer of mouse endothelial cells (H5V) in Transwell plate inserts (Corning, Corning, NY). The *mdx* (DYS GFP PB) MABs migrated on the other side of the filter were counted 11 hr after seeding (10 random fields at 10× magnification under a fluorescence microscope).

Satellite Cell Isolation

Satellite cells were isolated from TA muscles of *mdx* SCID mice transplanted with *mdx* (DYS GFP PB) MABs 90 days after transplantation, as described previously.[51] In brief, muscles were minced and

resuspended in 700–800 U/mL of collagenase II solution for 30 min and then washed in Ham's F10, 10% horse serum, 100 IU/L penicillin, and 100 mg/mL streptomycin medium. A second digestion with collagenase II (1,000 U/mL) and dispase II (11 U/mL) followed, after which the suspension was strained through 70 μm and 40 μm strainers (Falcon, Corning, NY) and collected in the wash medium. The cell suspension was then stained with antibodies for Integrin α-7 (Miltenyi Biotec, Bergisch Gladbach, Germany) recognized by an anti-mouse immunoglobulin G (IgG) conjugated with PE/Cy7 (R&D Systems), Sca-1 conjugated with BV421(R&D Systems), CD45, CD31, and CD11b conjugated with Allophycocyanin (R&D Systems). The cells were sorted in a cell sorter (BD FACS AriaII) to recover fractions that were positive for Integrin α-7 and GFP and negative for Sca-1, CD45, CD31, and CD11b and were used for DNA or RNA purifications. Alternatively, the percentage of GFP-positive satellite-like cells was assayed by flow cytometry (BD LSRII), as assessed by the expression of Integrin α-7 and GFP and the lack of CD45, CD31, Sca-1, and CD11b markers. Also, the quality of the satellite cell preparation was assessed by immunostaining for Pax7 on the isolated satellite cells.

Histology and Histochemistry

Muscle tissues were embedded in tragacanth gum and frozen in liquid nitrogen-cooled isopentane. Cryostat sections, 8 μm thick, were prepared with a Leica cryostat 1860UV (Leica, Richmond, IL), fixed with 4% paraformaldehyde, washed, and permeabilized in PBS containing 1% BSA and 0.2% (w/v) Triton X-100, followed by 1 hr of blocking with 10% goat serum at room temperature. Immunofluorescence staining was performed by overnight incubation at 4°C with the following primary antibodies: Mouse anti-dystrophin DYS1 and DYS2 1:40 (Novocastra, Newcastle upon Tyne, UK), rabbit anti-laminin 1:100 (Sigma), chicken anti-GFP 1:1,000 (Abcam, Cambridge, UK), mouse anti-β-galactosidase 1:100 (Abnova), mouse anti-myosin heavy chain 1:200 (eBioscience, Thermo Fisher Scientific, Lafayette, CO), α-sarcoglycan 1:100 (Novocastra), β-sarcoglycan 1:100 (Novocastra), β-dystroglycan 1:100 (Novocastra), n-nitric oxide synthase 1:100 (nNOS) (Invitrogen), syntrophin 1:100 (Invitrogen). For anti-mouse Pax7 (R&D Systems) immunostaining, samples were first stained with the required primary antibodies other than Pax7. Samples were then immersed in sodium citrate buffer (10 mM [pH 6.0]) at 100°C for demasking the antigen epitopes and incubated overnight at 4°C with anti-mouse Pax7. After incubation with primary antibodies, the samples were washed with 0.2% Triton X-100 PBS and then incubated with the secondary goat antibodies 1:500 (Invitrogen) for 1 hr. After three washes, slides were mounted using fluorescent mounting medium containing DAPI (Southern Biotech, Birmingham, AL) and observed under a fluorescence microscope (Leica-DM5500/Olympus Slidescanner VS120-L100).

Cryostat sections were used for H&E (Sigma) staining, X-gal staining (Invitrogen), and Masson trichome staining (Sigma) using standard protocols. The slides were then observed under microscopes and images were captured for further analysis (Leica DM5500/Olympus SlideScanner VS120-L100).

Image analysis was performed using ImageJ software (NIH, Bethesda, MD). For quantification of number of dystrophin-positive fibers per muscle cross-section, images of the whole cross-section were generated using an Olympus SlideScanner (Olympus, Tokyo, Japan). Numbers of dystrophin-positive fibers were counted using the cell counter plugin of ImageJ. For each muscle, fibers were counted at seven different distances (2 to 8 mm) from the distal tendon. Final calculations were made using the values obtained from four to eight muscles per group. Cross-sectional area (CSA) was measured by tracing transversal myofibers with the freehand selection tool and fiber area measured with the measurement analysis tool. Random fields were chosen from images of the whole cross-section made using a slide scanner (Olympus SlideScanner), and at least 150 myofibers per cross-section were counted. Between four and eight muscles were analyzed per condition, and plots of the CSA distribution were made using GraphPad Prism (GraphPad, San Diego, CA). Presence of fibrotic, adipose, scar tissue, and infiltrates was evaluated using the same images. This analysis was performed by separating the hematoxylin component and eosin component of the images and calculating the percentage of area occupied by the infiltrating material. This analysis gave an estimate of muscle damage in the treated muscles as compared to the controls.

Tumorigenesis Assay

In order to exclude potential tumorigenic mutations due to transposon vector integration events, CD1 nude mice (n = 8 per group) were injected subcutaneously in the dorsal flank, with 2,000,000 *mdx* (DYS GFP PB) MABs resuspended in 100 μL of calcium magnesium free PBS. As controls, one group of mice was injected with the same number of HeLa cells as positive control for tumor formation, another group was injected with untransfected *mdx* MABs, and a third group was mock-injected with PBS. The mice were monitored for any detectable tumor masses for 8 months after cell transplantations. The positive control, HeLa cell-injected mice, developed tumors within 1 month after injections, whereas the other test mice did not display any tumor.

PCR and Gene Copy Number Assays

DNA from MABs and mouse muscles was purified using the DNeasy Blood & Tissue Kit (QIAGEN, Hilden, Germany) as per the manufacturer's instructions. RNA was purified from MABs using NucleoSpin RNA kit (Macherey Nagel, Düren, Germany) and from mouse muscles using RNeasy Fibrous Tissue Mini Kit (QIAGEN). cDNA was prepared from 500 ng of each RNA sample using the GoScript Reverse Transcription System (Promega, Madison, WI). PCR on mouse muscle genomic DNA and MABs DNA and RT-PCR on mouse cDNA was carried out using Q5 High-Fidelity DNA Polymerase (New England Biolabs, Ipswich, MA) according to standard protocols. Endpoint PCR analysis was carried out to detect different regions on the human dystrophin coding sequence using primers enlisted as hDYS1, hDYS2, and hDYS3 (Table S1A). The primers (Microsynth, Baglach, Switzerland) used for the different PCRs, quantitative PCR (qPCR) with reverse transcription (RT-qPCR), for transgene copy number or relative RNA level assays, have been listed

in Table S1. qPCR and RT-qPCR amplifications were carried out using the LightCycler 480 SYBR Green I Master mix (Roche, Basel, Switzerland) and the ABI/Prism 7900 HT Thermocycler. Each DNA or cDNA sample was amplified in triplicate, and cDNA levels were normalized to that of the housekeeping gene encoding TATA-binding protein (TBP), by the comparative threshold cycle (Ct) method. Fold changes were determined using the Equation $2^{-\Delta\Delta Ct}$. Transposon copy number was quantified by methods of serial dilution,[52] relative to a reference gene present as one copy per haploid genome (TBP), and by whole-genome sequencing coverage. The primers used for this were on the dystrophin region (Table S1).

Genome Sequencing and Analysis

High molecular weight DNA was isolated from *mdx* (DYS PB) MABs using Blood & Cell Culture DNA Mini Kit (QIAGEN). Whole-genome sequencing of *mdx* (DYS PB) MABs was carried out by the Genomic Technologies Facility of University of Lausanne using the single-molecule, real-time (SMRT) sequencing technology (Pacific Biosciences, Menlo Park, CA). The data derived from 18 SMRT cells yielded a genome coverage of approximately 7.7-fold from high-quality sequences, which was then used to detect dystrophin integration sites mediated by the transposase, as described previously.[53] Integration events were retrieved using a threshold of more than 10 kb regions of similarity to the transposon sequence to identify reads spanning both extremities of transposon inserts. At least one of the two transposon borders could be characterized and found to contain the TTAA signature sequence indicative of PB transposition at the junction with the mouse genome, thus confirming that the integration events were transposase mediated.

Western Blot

Frozen tissues were prepared and used for immunoblotting as described previously.[54,55] Muscle extracts (3–30 μg/lane) were resolved by SDS-PAGE, and proteins were transferred onto nitrocellulose membranes according to standard procedures. Membranes were blocked for 1 hr in TBST (20 mmol/L Tris-base, 150 mmol/L NaCl, 0.1% Tween 20 [pH 7.5]) containing 5% nonfat dry milk and incubated overnight at 4°C with a primary antibody (mouse anti-dystrophin MANDYS8, Thermo Fisher; mouse anti-alpha-actinin, Sigma). After extensive washing, membranes were incubated for 1 hr with the appropriate horseradish peroxidase-conjugated secondary antibody in TBST containing 5% milk. Detection was done by chemiluminescence (ECL plus kit; Amersham, Little Chalfont, UK) using Fusion Pulse. Densitometric analysis was performed with ImageJ software. Signals were normalized to the alpha-actinin content.

Assessment of Muscle Function *In Situ*

At the end of the treatment period, the contractile properties of the TA were measured *in situ* essentially as described elsewhere.[37,54,55] In brief, mice were deeply anesthetized, the knee joint was immobilized, the distal tendon of the TA was attached to a force transducer, IM electrodes were inserted, and the tension developed by the TA in response to 0.5-ms-long electrical stimulations was recorded isometrically. The fatigability of the TA exposed to repetitive maximal tetanic contractions was determined: the TAs were stimulated at 200 Hz for 200 ms, resulting in fused tetani. A total of 20 tetani were delivered at 30 s intervals. The force generated at every tetanus was expressed as the percentage of the initial force. The extent of force loss was calculated from the force remaining at the end of the assay.

AFM Assays

The restoration of the resistance to elastic deformation of individual dystrophin-expressing myofibers was assessed using AFM as described previously.[37] After mouse sacrifice, the TA muscles were dissected out and immediately frozen in liquid-nitrogen-cooled isopentane and stored at −70°C until thawing for use in AFM assays. Before performing measurements, a 1-mm-thick section of the muscle was cut and glued onto a glass coverslip using two 0.5-μL droplets of cyanoacrylate adhesive (AXIA) placed at both extremities of the muscle slice. The slice was immediately immersed in DMEM and AFM measurements were performed. One hundred to three hundred locations were assayed on each muscle slice. AFM assays were performed using a commercially available device (PSIA XE120, Park Systems, Korea) equipped with the "liquid cell" setup. Standard silicon nitride gold-coated cantilevers (ORC8, Bruker) with a nominal spring constant value of 0.38 N/m were used in all measurements. To determine the mean value of the Young's modulus (calculated for the indentation depth of 200 nm), the modulus distribution was fitted with the Gaussian function. The center of the distribution corresponds to the mean value, while half of its width, taken at half height, denotes the standard deviation.

Statistical Analysis

Data were analyzed using GraphPad Prism 7 and Microsoft Excel. Results were represented as mean ± SD. Statistical analyses were performed using the Mann-Whitney tests for significance of differences. *P* values lower than 0.05 were considered as significant.

SUPPLEMENTAL INFORMATION

Supplemental Information includes eleven figures and one table and can be found with this article online at https://doi.org/10.1016/j.ymthe.2018.01.021.

AUTHOR CONTRIBUTIONS

Conceptualization and Experiment Design, N.M., P.S.I.; Funding Acquisition, N.M.; Manuscript Writing, P.S.I., N.M.; Data Analysis, P.S.I., L.O.M., E.S.-S., J.Z., O.M.D., M.L.; Performing of Experiments, P.S.I., L.O.M., F.R., J.Z., S.A., L.A.N., O.M.D.; Supervision and Comments, N.M., M.L., M.J., G.M., O.M.D.

CONFLICTS OF INTEREST

The authors declare no conflict of interest.

ACKNOWLEDGMENTS

The authors are grateful to Jacques Tremblay for the kind gift of plasmids, to Denis Fahmi for expert technical assistance, to Roy Combe, Arnaud Bichat, and Francis Derouet for expert animal care and surgery, and to the Vital-IT computer cluster for genomic data handling

and analysis. This work was supported by grants from the Swiss Foundation for Research on Muscle Diseases to N.M. and the Universities of Lausanne and Geneva.

REFERENCES

1. Fairclough, R.J., Wood, M.J., and Davies, K.E. (2013). Therapy for Duchenne muscular dystrophy: renewed optimism from genetic approaches. Nat. Rev. Genet. *14*, 373–378.
2. Hoffman, E.P., Brown, R.H., Jr., and Kunkel, L.M. (1987). Dystrophin: the protein product of the Duchenne muscular dystrophy locus. Cell *51*, 919–928.
3. Davies, K.E., and Nowak, K.J. (2006). Molecular mechanisms of muscular dystrophies: old and new players. Nat. Rev. Mol. Cell Biol. *7*, 762–773.
4. Manzur, A.Y., and Muntoni, F. (2009). Diagnosis and new treatments in muscular dystrophies. Postgrad. Med. J. *85*, 622–630.
5. Muntoni, F., Torelli, S., and Ferlini, A. (2003). Dystrophin and mutations: one gene, several proteins, multiple phenotypes. Lancet Neurol. *2*, 731–740.
6. Aartsma-Rus, A., and Krieg, A.M. (2017). FDA approves eteplirsen for Duchenne muscular dystrophy: the next chapter in the eteplirsen saga. Nucleic Acid Ther. *27*, 1–3.
7. Echigoya, Y., Aoki, Y., Miskew, B., Panesar, D., Touznik, A., Nagata, T., Tanihata, J., Nakamura, A., Nagaraju, K., and Yokota, T. (2015). Long-term efficacy of systemic multiexon skipping targeting dystrophin exons 45-55 with a cocktail of vivo-morpholinos in mdx52 mice. Mol. Ther. Nucleic Acids *4*, e225.
8. Echigoya, Y., Nakamura, A., Nagata, T., Urasawa, N., Lim, K.R.Q., Trieu, N., Panesar, D., Kuraoka, M., Moulton, H.M., Saito, T., et al. (2017). Effects of systemic multiexon skipping with peptide-conjugated morpholinos in the heart of a dog model of Duchenne muscular dystrophy. Proc. Natl. Acad. Sci. USA *114*, 4213–4218.
9. Tedesco, F.S., Dellavalle, A., Diaz-manera, J., Messina, G., and Cossu, G. (2010). Repairing skeletal muscle: regenerative potential of skeletal muscle stem cells. J. Clin. Invest. *120*, 11–19.
10. Puttini, S., van Zwieten, R.W., Saugy, D., Lekka, M., Hogger, F., Ley, D., Kulik, A.J., and Mermod, N. (2013). MAR-mediated integration of plasmid vectors for in vivo gene transfer and regulation. BMC Mol. Biol. *14*, 26.
11. Gregorevic, P., Blankinship, M.J., Allen, J.M., Crawford, R.W., Meuse, L., Miller, D.G., Russell, D.W., and Chamberlain, J.S. (2004). Systemic delivery of genes to striated muscles using adeno-associated viral vectors. Nat. Med. *10*, 828–834.
12. Tedesco, F.S., Hoshiya, H., D'Antona, G., Gerli, M.F., Messina, G., Antonini, S., Tonlorenzi, R., Benedetti, S., Berghella, L., Torrente, Y., et al. (2011). Stem cell-mediated transfer of a human artificial chromosome ameliorates muscular dystrophy. Sci. Transl. Med. *3*, 96ra78.
13. Tedesco, F.S. (2015). Human artificial chromosomes for Duchenne muscular dystrophy and beyond: challenges and hopes. Chromosome Res. *23*, 135–141.
14. Xu, L., Park, K.H., Zhao, L., Xu, J., El Refaey, M., Gao, Y., Zhu, H., Ma, J., and Han, R. (2016). CRISPR-mediated genome editing restores dystrophin expression and function in mdx mice. Mol. Ther. *24*, 564–569.
15. Nelson, C.E., Hakim, C.H., Ousterout, D.G., Thakore, P.I., Moreb, E.A., Castellanos Rivera, R.M., Madhavan, S., Pan, X., Ran, F.A., Yan, Y.X., et al. (2016). In vivo genome editing improves muscle function in a mouse model of Duchenne muscular dystrophy. Science *351*, 403–407.
16. Long, C., Amoasii, L., Mireault, A.A., McAnally, J.R., Li, H., Sanchez-Ortiz, E., Bhattacharyya, S., Shelton, J.M., Bassel-Duby, R., and Olson, E.N. (2016). Postnatal genome editing partially restores dystrophin expression in a mouse model of muscular dystrophy. Science *351*, 400–403.
17. Tabebordbar, M., Zhu, K., Cheng, J.K.W., Chew, W.L., Widrick, J.J., Wan, W.X., Maesner, C., Wu, E.Y., Xiao, R., Ran, F.A., et al. (2015). In vivo gene editing in dystrophic mouse muscle and muscle stem cells. Science *351*, 407–411.
18. Li, S., Kimura, E., Ng, R., Fall, B.M., Meuse, L., Reyes, M., Faulkner, J.A., and Chamberlain, J.S. (2006). A highly functional mini-dystrophin/GFP fusion gene for cell and gene therapy studies of Duchenne muscular dystrophy. Hum. Mol. Genet. *15*, 1610–1622.
19. Aartsma-Rus, A., and van Ommen, G.-J.B. (2009). Less is more: therapeutic exon skipping for Duchenne muscular dystrophy. Lancet Neurol. *8*, 873–875.
20. Mann, C.J., Honeyman, K., Cheng, A.J., Ly, T., Lloyd, F., Fletcher, S., Morgan, J.E., Partridge, T.A., and Wilton, S.D. (2001). Antisense-induced exon skipping and synthesis of dystrophin in the mdx mouse. Proc. Natl. Acad. Sci. USA *98*, 42–47.
21. Miura, P., and Jasmin, B.J. (2006). Utrophin upregulation for treating Duchenne or Becker muscular dystrophy: how close are we? Trends Mol. Med. *12*, 122–129.
22. Tinsley, J., Robinson, N., and Davies, K.E. (2015). Safety, tolerability, and pharmacokinetics of SMT C1100, a 2-arylbenzoxazole utrophin modulator, following single- and multiple-dose administration to healthy male adult volunteers. J. Clin. Pharmacol. *55*, 698–707.
23. Kim, A., and Pyykko, I. (2011). Size matters: versatile use of PiggyBac transposons as a genetic manipulation tool. Mol. Cell. Biochem. *354*, 301–309.
24. Li, M.A., Turner, D.J., Ning, Z., Yusa, K., Liang, Q., Eckert, S., Rad, L., Fitzgerald, T.W., Craig, N.L., and Bradley, A. (2011). Mobilization of giant piggyBac transposons in the mouse genome. Nucleic Acids Res. *39*, e148.
25. Muses, S., Morgan, J.E., and Wells, D.J. (2011). Restoration of dystrophin expression using the Sleeping beauty transposon. PLoS Curr. *3*, RRN1296.
26. Escobar, H., Schöwel, V., Spuler, S., Marg, A., and Izsvák, Z. (2016). Full-length dysferlin transfer by the hyperactive Sleeping Beauty transposase restores dysferlin-deficient muscle. Mol. Ther. Nucleic Acids *5*, e277.
27. Hudecek, M., Izsvák, Z., Johnen, S., Renner, M., Thumann, G., and Ivics, Z. (2017). Going non-viral: the *Sleeping Beauty* transposon system breaks on through to the clinical side. Crit. Rev. Biochem. Mol. Biol. *52*, 355–380.
28. Loperfido, M., Jarmin, S., Dastidar, S., Di Matteo, M., Perini, I., Moore, M., Nair, N., Samara-Kuko, E., Athanasopoulos, T., Tedesco, F.S., et al. (2016). piggyBac transposons expressing full-length human dystrophin enable genetic correction of dystrophic mesoangioblasts. Nucleic Acids Res. *44*, 744–760.
29. Ding, S., Wu, X., Li, G., Han, M., Zhuang, Y., and Xu, T. (2005). Efficient transposition of the piggyBac (PB) transposon in mammalian cells and mice. Cell *122*, 473–483.
30. Wilson, M.H., Coates, C.J., and George, A.L., Jr. (2007). PiggyBac transposon-mediated gene transfer in human cells. Mol. Ther. *15*, 139–145.
31. Ley, D., Van Zwieten, R., Puttini, S., Iyer, P., Cochard, A., and Mermod, N. (2014). A PiggyBac-mediated approach for muscle gene transfer or cell therapy. Stem Cell Res. (Amst.) *13*, 390–403.
32. Cossu, G., and Bianco, P. (2003). Mesoangioblasts—vascular progenitors for extravascular mesodermal tissues. Curr. Opin. Genet. Dev. *13*, 537–542.
33. Sampaolesi, M., Torrente, Y., Innocenzi, A., Tonlorenzi, R., D'Antona, G., Pellegrino, M.A., Barresi, R., Bresolin, N., De Angelis, M.G., Campbell, K.P., et al. (2003). Cell therapy of alpha-sarcoglycan null dystrophic mice through intra-arterial delivery of mesoangioblasts. Science *301*, 487–492.
34. Sampaolesi, M., Blot, S., D'Antona, G., Granger, N., Tonlorenzi, R., Innocenzi, A., Mognol, P., Thibaud, J.L., Galvez, B.G., Barthélémy, I., et al. (2006). Mesoangioblast stem cells ameliorate muscle function in dystrophic dogs. Nature *444*, 574–579.
35. Cossu, G., Previtali, S.C., Napolitano, S., Cicalese, M.P., Tedesco, F.S., Nicastro, F., Noviello, M., Roostalu, U., Natali Sora, M.G., Scarlato, M., et al. (2015). Intra-arterial transplantation of HLA-matched donor mesoangioblasts in Duchenne muscular dystrophy. EMBO Mol. Med. *7*, 1513–1528.
36. van Zwieten, R.W., Puttini, S., Lekka, M., Witz, G., Gicquel-Zouida, E., Richard, I., Lobrinus, J.A., Chevalley, F., Brune, H., Dietler, G., et al. (2014). Assessing dystrophies and other muscle diseases at the nanometer scale by atomic force microscopy. Nanomedicine (Lond.) *9*, 393–406.
37. Puttini, S., Lekka, M., Dorchies, O.M., Saugy, D., Incitti, T., Ruegg, U.T., Bozzoni, I., Kulik, A.J., and Mermod, N. (2009). Gene-mediated restoration of normal myofiber elasticity in dystrophic muscles. Mol. Ther. *17*, 19–25.
38. Neri, M., Torelli, S., Brown, S., Ugo, I., Sabatelli, P., Merlini, L., Spitali, P., Rimessi, P., Gualandi, F., Sewry, C., et al. (2007). Dystrophin levels as low as 30% are sufficient to avoid muscular dystrophy in the human. Neuromuscul. Disord. *17*, 913–918.
39. Tedesco, F.S., and Cossu, G. (2012). Stem cell therapies for muscle disorders. Curr. Opin. Neurol. *25*, 597–603.

40. Roca, I., Requena, J., Edel, M.J., and Alvarez-Palomo, A.B. (2015). Myogenic precursors from iPS cells for skeletal muscle cell replacement therapy. J. Clin. Med. *4*, 243–259.

41. Pichavant, C., Chapdelaine, P., Cerri, D.G., Bizario, J.C.S., and Tremblay, J.P. (2010). Electrotransfer of the full-length dog dystrophin into mouse and dystrophic dog muscles. Hum. Gene Ther. *21*, 1591–1601.

42. Henssen, A.G., Henaff, E., Jiang, E., Eisenberg, A.R., Carson, J.R., Villasante, C.M., Ray, M., Still, E., Burns, M., Gandara, J., et al. (2015). Genomic DNA transposition induced by human PGBD5. eLife *4*, 1–20.

43. Ivics, Z. (2016). Endogenous transposase source in human cells mobilizes piggyBac transposons. Mol. Ther. *24*, 851–854.

44. Galvan, D.L., Nakazawa, Y., Kaja, A., Kettlun, C., Cooper, L.J., Rooney, C.M., and Wilson, M.H. (2009). Genome-wide mapping of PiggyBac transposon integrations in primary human T cells. J. Immunother. *32*, 837–844.

45. Chamberlain, J.S. (1997). Dystrophin levels required for genetic correction of Duchenne muscular dystrophy. Basic Appl. Myol. *7*, 251–256.

46. Quattrocelli, M., Palazzolo, G., Perini, I., Crippa, S., Cassano, M., and Sampaolesi, M. (2012). Mouse and human mesoangioblasts: isolation and characterization from adult skeletal muscles. Methods Mol. Biol. *798*, 65–76.

47. Filareto, A., Parker, S., Darabi, R., Borges, L., Iacovino, M., Schaaf, T., Mayerhofer, T., Chamberlain, J.S., Ervasti, J.M., McIvor, R.S., et al. (2013). An ex vivo gene therapy approach to treat muscular dystrophy using inducible pluripotent stem cells. Nat. Commun. *4*, 1549.

48. Bonfanti, C., Rossi, G., Tedesco, F.S., Giannotta, M., Benedetti, S., Tonlorenzi, R., Antonini, S., Marazzi, G., Dejana, E., Sassoon, D., et al. (2015). PW1/Peg3 expression regulates key properties that determine mesoangioblast stem cell competence. Nat. Commun. *6*, 6364.

49. Acsadi, G., Dickson, G., Love, D.R., Jani, A., Walsh, F.S., Gurusinghe, A., Wolff, J.A., and Davies, K.E. (1991). Human dystrophin expression in mdx mice after intramuscular injection of DNA constructs. Nature *352*, 815–818.

50. Wang, B., Li, J., and Xiao, X. (2000). Adeno-associated virus vector carrying human minidystrophin genes effectively ameliorates muscular dystrophy in mdx mouse model. Proc. Natl. Acad. Sci. USA *97*, 13714–13719.

51. Liu, L., Cheung, T.H., Charville, G.W., and Rando, T.A. (2015). Isolation of skeletal muscle stem cells by fluorescence-activated cell sorting. Nat. Protoc. *10*, 1612–1624.

52. Di Matteo, M., Samara-Kuko, E., Ward, N.J., Waddington, S.N., McVey, J.H., Chuah, M.K., and VandenDriessche, T. (2014). Hyperactive piggyBac transposons for sustained and robust liver-targeted gene therapy. Mol. Ther. *22*, 1614–1624.

53. Kostyrko, K., Neuenschwander, S., Junier, T., Regamey, A., Iseli, C., Schmid-Siegert, E., Bosshard, S., Majocchi, S., Le Fourn, V., Girod, P.A., et al. (2017). MAR-Mediated transgene integration into permissive chromatin and increased expression by recombination pathway engineering. Biotechnol. Bioeng. *114*, 384–396.

54. Dorchies, O.M., Reutenauer-Patte, J., Dahmane, E., Ismail, H.M., Petermann, O., Patthey- Vuadens, O., Comyn, S.A., Gayi, E., Piacenza, T., Handa, R.J., et al. (2013). The anticancer drug tamoxifen counteracts the pathology in a mouse model of duchenne muscular dystrophy. Am. J. Pathol. *182*, 485–504.

55. Reutenauer-Patte, J., Boittin, F.X., Patthey-Vuadens, O., Ruegg, U.T., and Dorchies, O.M. (2012). Urocortins improve dystrophic skeletal muscle structure and function through both PKA- and Epac-dependent pathways. Am. J. Pathol. *180*, 749–762.